Therapeutic targeting of sunitinib-induced AR phosphorylation in renal cell carcinoma

Remi Adelaiye-Ogala[1,2#], Nur P Damayanti[1#], Ashley R. Orillion[1,3], Sreevani Arisa[1], Sreenivasulu Chintala[1], Mark A. Titus[4], Chinghai Kao[5], and Roberto Pili[1,5*]

[1]Genitourinary Program, Simon Cancer Center, Indiana University, Indianapolis, IN USA;[2]Department of Cancer Pathology and Prevention, University at Buffalo, Roswell Park Cancer Institute, Buffalo, NY USA;[3]Department of Cellular and Molecular Biology, University at Buffalo, Roswell Park Cancer Institute, Buffalo, NY USA;[4]Department of Genitourinary Oncology, MD Anderson, Houston, TX, [5]Department of Urology, Indiana University, Indianapolis, IN USA

Running Title: AR phosphorylation and sunitinib resistance in RCC

Key Words: Renal cell carcinoma, sunitinib resistance, androgen receptor

Conflict of interest: The authors declare no conflict of interest.

# These authors contributed equally

****Corresponding Author***
Roberto Pili, MD
Genitourinary Program,
Indiana University-Simon Cancer Center
Indianapolis, IN
rpili@iu.edu

Statement of significance

Findings highlight the therapeutic potential of targeting the androgen receptor to overcome RCC resistance to receptor tyrosine kinase inhibitors.

This is the author's manuscript of the article published in final edited form as:

Adelaiye-Ogala, R., Damayanti, N. P., Orillion, A. R., Arisa, S., Chintala, S., Titus, M. A., … Pili, R. (2018). Therapeutic Targeting of Sunitinib-Induced AR Phosphorylation in Renal Cell Carcinoma. Cancer Research, 78(11), 2886–2896. https://doi.org/10.1158/0008-5472.CAN-17-3386

Abstract

Androgen receptor (AR) plays a crucial role in the development and progression of prostate cancer. AR expression has also been reported in other solid tumors, including renal cell carcinoma (RCC), but its biological role here remains unclear. Through integrative analysis of a reverse phase protein array (RPPA), we discovered increased expression of AR in an RCC patient-derived xenograft model of acquired resistance to the receptor tyrosine kinase inhibitor (RTKi) sunitinib. AR expression was increased in RCC cell lines with either acquired or intrinsic sunitinib resistance *in vitro*. An AR signaling gene array profiler indicated elevated levels of AR target genes in sunitinib-resistant cells. Sunitinib-induced AR transcriptional activity was associated with increased phosphorylation of serine 81 (pS81) on AR. Additionally, AR overexpression resulted in acquired sunitinib resistance, and the AR antagonist enzalutamide-induced AR degradation and attenuated AR downstream activity in sunitinib-resistant cells, also indicated by decreased secretion of human kallikrein 2 (KLK2). Enzalutamide-induced AR degradation was rescued by either proteasome inhibition or by knockdown of the AR ubiquitin ligase speckle-type POZ protein (SPOP). *In vivo* treatment with enzalutamide and sunitinib demonstrated that this combination efficiently induced tumor regression in an RCC model following acquired sunitinib resistance. Overall, our results suggest the potential role of AR as a target for therapeutic interventions, in combination with RTKi, to overcome drug resistance in RCC.

Introduction

Androgen receptor (AR) plays a crucial role in the development and progression of prostate cancer (1). AR expression has also been reported in other solid tumors, including renal cell carcinoma (RCC) (2-6). AR signaling has been reported to promote progression in RCC *via* the HIF-2α/VEGF signaling pathway, by recruiting vascular endothelial cells (5), and by altering the AKT/NF-kB signaling axis (7). However, AR has also been reported to potentially be a good outcome prognosticator in a retrospective analysis of RCC patients (8), suggesting that the biological role played by AR in RCC remains unclear.

Although AR is activated by ligand binding in prostate cancer, recent reports have identified several post-translational modifications, including AR phosphorylation, that alter AR activity (9). Most of the identified phospho-sites in full length AR lay in the serine and tyrosine residues, and the phosphorylation of these sites have been implicated in several different cellular responses, including AR expression and transcriptional activity (10,11). Members of the Src family may facilitate AR activation through direct phosphorylation of pY534/267, and inhibition of these kinases abrogated AR phosphorylation and induced tumor cell regression in prostate cancer models (12,13). Similarly, phosphorylation and stabilization of AR by cyclin-dependent kinase 1 (CDK1) has been reported in prostate cancer (14). Phosphorylation of pS81, by CDK1, leads to the activation of AR and inhibition of this kinase decreased AR pS81 and AR activity (14). Other reports have shown that AR can be either activated, or inhibited, *via* AKT mediated pS213/791 phosphorylation (15-17). Interestingly, it is known that most of AR phosphorylation occur in tumors with low androgen levels (18), and renal cell carcinoma has been reported to have very low levels of androgens (19).

Enzalutamide is a second generation AR antagonist that inhibits AR-ligand interaction and AR transcriptional activity, and has been approved for the treatment of castration-resistant prostate cancer (20) (21). Receptor tyrosine kinase inhibitors (RTKIs) such as sunitinib, pazopanib and axitinib are effective treatments for clear cell renal cell carcinoma (ccRCC) patients (22). New RTKIs, such as cabozantinib (23,24) and lenvatinib (25), have been recently approved in the first and second line setting, respectively. However, resistance to RTKIs represents a major hurdle in the clinical management of advanced ccRCC. Despite the clinical benefit, generally acquired resistance to RTKIs occurs within 12 months in the first line setting. Several potential mechanisms have been identified to play a role in drug resistance, including upregulation of alternative pathways (22) (26) (27). Our group has recently reported that epigenetic tumor cell adaptation to RTKis may lead to kinome reprogramming, as well as increased global serine and tyrosine phosphorylation (28). Thus, the identification of specific, "druggable" targets may delay/overcome the occurrence of drug resistance and prolong the clinical benefit of RTKis in RCC.

Here, we report the role of AR and its association with resistance to RTKis in RCC models. Furthermore, we show that sunitinib promotes AR activation *via* increased phosphorylation, and the AR antagonist, enzalutamide, restores sensitivity to sunitinib by inducing SPOP-mediated AR degradation.

Materials and methods

In vivo and in vitro studies

In vitro assays were performed using commercially available RCC cell lines 786-0, UMRC2, ACHN, Caki2 (ATCC) and lab-generated 786-0R (acquired sunitinib resistant). Cells were maintained and cultured in the appropriate media, supplemented with 10% FBS and 1% penicillin and streptomycin. All cells are routinely tested and checked for the absence of mycoplasma. Authentication was conducted by Multiplex 10 STRs loci detection method (ATCC). For transient transfection, cells were transfected with 50nM siSPOP (Ambion) or siControl(Ambion) using Lipofectamine 2000 transfection reagent, according to manufacturer's protocol (cat#:11668027, ThermoFisher Scientific). For treatment, cells were plated in 24 well plated and 24 hours post seeding cells were treated with either sunitinib (5uM, LC laboratories), enzalutamide (500nM, Selleckchem), axitinib (5μM, LC laboratories) or MG-132 (10μM, Selleckchem) or combinations, for either 24, 48 or 72 hours. Crystal violet assay (Sigma) was used to evaluate cells growth after different time point-treatment, and absorbance was read using a spectrometer (xMarks Spectrometer, Bio-Rad). For *in vivo* studies, 786-0 (sunitinib sensitive) and RP-R-02LM (sunitinib resistant) models were used. All *in vivo* experiments were approved and performed in strict accordance with the guidelines of the Institutional Animal Care and Use Committee (IACUC) at Indiana University, Indianapolis IN. 786-0 and RP-R-02LM viable tumors were selected, dissected into ~1mm^2 tumor pieces, and implanted subcutaneously into six-week-old homozygous ICR, Severe Combined Immune-deficient (SCID) female mice. All mice were operated under sedation with oxygen, isoflurane and buprenorphine. When tumors were established, and reached 50mm^2, mice were randomly grouped and placed in either control group or treatment groups (n=5-10). Mice received sunitinib treatment (40mg/kg 5days on, 2

days off, PO), enzalutamide (MDV300) treatment (10mg/kg, PO), or a combination of both. Tumor burden was assessed once a week by caliper measurement of two diameters of the tumor (L x W = mm2) and reported as tumor volume ((L X W2)/2 = mm^3). Body weights and endpoint tumor weights were assessed using a weighing scale and recorded in grams. Tissue and blood were collected under aseptic conditions. 1 ml of blood was collected by cardiac bleeds (terminal) at the end of the experiment. Serum and plasma were separated, and aliquots were stored at -80C for further analysis. Tumor tissues were excised, cut into sections and were snap-frozen and stored in -80C, fixed in 10% buffered formalin, or zinc for histopathology and saved in trizol for RNA analysis.

Steroid quantitation

Steroid standards, dihydrotestosterone, progesterone, testosterone and epi-testosterone were purchased from Steraloids (Newport, RI). Steroid $^{13}C_3$-internal-standards were purchased from IsoSciences (King of Prussia, PA). Hydroxylamine hydrochloride, ultrapure methanol and water (Chromasolv) were purchased from Sigma-Aldrich (St Louis, MO). Steroids were extracted from sample homogenates after addition of internal-standard (0.5 ng each) using tert-butyl methyl ether, and the separated organic layer was evaporated. The extracts were subsequently derivatized using hydroxylamine hydrochloride in water/methanol (29). An Agilent 6495 triple quadrupole mass spectrometer (Santa Clara, CA), equipped with a Jet Stream electrospray ion source, a 1290 Infinity II ultrahigh-performance liquid chromatography system, and MassHunter Workstation software was used to quantify steroids. Chromatographic separation of testosterone, epi-testosterone, dihydrotestosterone and progesterone oximes result in elution at 3.4, 3.6, 3.9 and 4.3 minutes, respectively. Molecular ion transitions monitored for progesterone (*m/z* 345.2 to 124.2), DHT (*m/z* 306.2 to 255.2), testosterone (*m/z* 304.2 to 124.1), epi-testosterone (304.2 to

124.1). The same ion transitions plus 3 mass units were monitored for $^{13}C_3$ internal-standards. The lower limit of quantification was 2.0 femtograms for testosterone, epi-testosterone and progesterone, and 25 femtograms for dihydrotestosterone.

Immunohistochemistry and immunofluorescence staining

Tissue specimens were fixed for 24 hours, paraffin embedded and sectioned (4μm). Immunohistochemistry (IHC) and immunofluorescence (IF) were performed using standard protocols. In brief, sections were de-paraffinized and rehydrated through graded alcohol washes. Antigen unmasking was achieved by boiling slides in either sodium citrate buffer (pH=6.0) or EDTA. To examine the expressions of our proteins of interests, tissue section was blocked with 2.5% horse serum (Vector Laboratories) and incubated overnight in primary antibodies against AR (1:1000; cat# 5153Cell Signaling). For IHC, following primary incubation, tissue sections were incubated in horseradish-conjugated anti-rabbit, according to manufacturer's protocol (Vector Laboratories), followed by enzymatic development in diaminobenzidine (DAB) and counter stained in hematoxylin. Sections were dehydrated and mounted with cytoseal 60 (ThermoScientific). For IF staining, sections were blocked with 5% BSA (Sigma), stained with either phospho-Tyrosine (1:50; sc-508, Santa Cruz), phospho-Serine (1:50, 600-401-26, Rockland, USA), or AR (1:400; 5153, Cell Signaling), AR-C19 (1:10; sc-815, Santa Cruz), Ki67 (1:10; MA5-14520, ThermoFisher), Tunel (cat # G3250, Promega), Phospho-AR (pS81) (1:50, 04-078, Millipore), and incubated overnight at 4C. Following primary incubation, sections were incubated with either Alexa Fluor or FITC fluorophores conjugated anti-rabbit (ThermoFisher) or anti-mouse (1:400; ThermoFisher) antibody, at room temperature in a humid light-tight box. Afterwards, slides were stained with actin green (1:10; cat#R37110, ThermoFisher), counter

stained with Hoechst (cat# 23491-45.4; SIGMA), and mounted with VectorShield mounting medium (Vector laboratories). Stained sections were analyzed either under bright field (IHC), or under appropriate fluorescence wavelength (IF) using the EVOS FL cell imaging microscope (Life Technology) and Leica Confocal microscope (Leica). The number of positive cells was determined in a blinded fashion, by analyzing four random 20x fields per tissue and quantified using Image J software.

RNA-sequencing and quantitative RT-PCR

RNA was extracted in accordance with manufacturer's protocol (miRNeasy; Qiagen), and RNA-sequencing was performed as previously described (25). In brief, RNA illumine sequencing reads were de-multiplex, aligned against human genome (hg19), and results aligned to BAM formatted sequence alignment map via cufflinks program. Differential expressed transcripts were identified between 786-0 and 786-0R samples, and ranked based on the square root of the sum of squares for the log2 fold change. For qRT-PCR analysis, gene expression assessment on AR target genes was performed using the Prime PCR array (Bio-Rad) according to manufacturer's protocol. AR primer used is forward primer; 5-*GGTGAGCAGAGTGCCCTATC*-3 and reverser primer; 5-*TCGGGTATTTCGCATGTCCC*-3. In brief, the denaturation step was carried out at 95C for 10 seconds; the annealing step was carried out at 58C for 30 seconds, and extension step at 72C for 1 minute using the applied Biosystems 7900HT fast real-time PCR system (Applied Biosystems). Sequence Detection Systems Software v2.3 was used to identify cycle threshold (Ct) values and generate gene expression curves. All data were normalized to either GAPDH expression.

Small interference RNA mediated SPOP silencing. UMR-C2 cells were transfected with either of two different siRNAs (Silencer® Select siRNAs, Sigma #4392420) targeting either exon 9-10 (id: s15954) or exon 10 (id: s15956) of *SPOP*. UMR-C2 cells were cultured in 6-well plates until 50%-60% confluence in antibiotic free RPMI-1641, transfected with SPOP-siRNA with final concentration 100 nM using Lipofectamine™ RNAiMAX Transfection Reagent (Invitrogen #13778075, USA) according to the manufacturer's instructions. At 72 h after transfection, cells were harvested for either immunoblotting or immunofluorescence analyses.

Western blotting

Whole cell protein extracts from tissue and cell were denatured, separated on SDS-PAGE gels and transferred to nitrocellulose membranes. After blocking in 5% enhanced blocking agent (GE) in Tris-buffered saline–Tween, membranes were probed overnight at 4°C with either, AR (1;1000; cat# 5153, Cell Signaling), SPOP (1:1000; ab168619, Abcam), or phospho-AR (S81) (1:1000; cell signaling, CA USA). After incubation with the appropriate secondary antibody, results were detected using Western Lightning Chemiluminescence Reagent Plus, according tothe manufacturer's instructions (ThermoFisher Scientific) and captured on film. Quantitative measurements of Western blot analysis were performed using ImageJ and Graph-Pad software (Prism 7).

Statistical analysis

Data analyses are expressed as the mean + standard error of mean (SEM). Statistical significance where appropriate was evaluated using a two-tailed student t test when comparing two groups, or by one-way analysis of variance (ANOVA), using the student-Newman Keuls post-test for

multiple comparison. A p value < 0.05, *p <0.05, **p < 0.01, ***p <0.001, was considered significant; ns= not significant. Statistical analyses were done by GraphPad software.

Results

AR expression is associated with acquired and intrinsic resistance to sunitinib. To identify potential markers associated with drug resistance in RCC, we recently performed a RPPA analysis in a patient-derived xenograft (PDX) model (RP-R-01), where *in vivo* transient acquired resistance to sunitinib was observed following chronic drug exposure (30). As expected, we detected dynamic changes in several proteins as tumors progressed from RTKi sensitivity to acquired resistance. To our surprise, among the protein changes, there was a significant increase ($p>0.05$) in AR expression in the sunitinib resistant tumors (**Fig. 1A**). We confirmed this finding by immunohistochemistry and qPCR in both RP-R-01 and RP-R-02 tumor models at the time of resistance to sunitinib (30), and in a derived metastatic model (RP-R-02LM) that is intrinsically resistant to sunitinib (28) (**Fig. 1B, C**). Thus, we analyzed gene and protein AR expression in the human RCC cell line 786-0 and its sunitinib resistant derivative (786-0R), and we detected a significant increase following chronic drug exposure (**Fig. 1D, E**). We also assessed AR expression in other RCC cell lines (**Fig. 1E**). We observed that AR levels correlated with sensitivity to sunitinib, showing higher IC50 in AR^+ RCC cell lines (786-0R, UMRC2 and Caki2) as compared to AR^- RCC cell lines (786-0, ACHN) (**Fig. 1F**). These data suggest that higher AR expression is associated with resistance to the direct anti-tumor effect of sunitinib. Thus, we tested whether inhibition of AR activity with the AR antagonist, enzalutamide, has biological activity in our RCC models. We treated AR^- 786-0 and ACHN, AR^+ 786-0R, UMRC2, and Caki2 cells with sunitinib, enzalutamide, or combination for 48 hours, and then performed a crystal violet assay. Quantitative analysis indicated a synergistic effect of enzalutamide and sunitinib in sunitinib resistant (AR^+), but not in sunitinib sensitive (AR^-), RCC cell lines (**Fig. 1G** and **Supplementary Fig. 1A, B**). Interestingly, single agent enzalutamide did not have a

significant effect on AR^+ 786-0R RCC cell viability, but the combination with sunitinib inhibited Ki67 expression (**Fig. 1H**). Similar results were obtained with another AR antagonist, bicalutamide, and also with axitinib, another RTKi approved for the treatment of RCC (**Supplementary Fig. 1C**). To further explore the contribution of AR in modulating resistance to sunitinib, we overexpressed AR^{wt} in 786-0 cells (AR^-) using a pEGFP-C1-AR expressing plasmid. Following 3 weeks of selection, we performed qRT-PCR to confirm successful transfection **(Supplementary Fig. 1D**), and conducted a sunitinib dose-response assay to determine whether AR overexpression decreased sensitivity to sunitinib. Interestingly, dose-response curves indicated a shift in the IC_{50} from 5.2μM in the 786-0 (parental) to 12.3μM in 786-0AR (**Fig. 1I**). In a separate experiment, the concomitant treatment with enzalutamide reverted in part the sunitinib sensitivity **(Supplementary Fig. 1E**). Taken together, these data suggest that AR expression modifies, in part, sunitinib resistance in RCC.

Sunitinib induces ligand-independent AR activation *via* S81 phosphorylation. To determine whether AR expression in our RCC models was associated with functional activity, we analyzed RNA-seq data and ran a gene array on AR signaling and AR targeted genes, comparing the AR^- sunitinib sensitive 786-0 cell line and the derived AR^+ sunitinib resistant 786-0R cell line. Indeed, the generated heat map indicated an increase in mRNA expression levels of AR targeted genes (i.e. *APPBP2*, *ZBTB16*, *KLK4*, *KLK2*, *TMPRSS2*), suggesting that sunitinib-induced AR is transcriptionally active (**Fig. 2A, B, Supplementary Fig. 2A-C**). To determine whether sunitinib has a direct effect on AR expression, we treated 786-0, 786-0R (after sunitinib washout for one week), and UMRC2 cells with sunitinib. Then, we examined gene expression of AR targeted genes in the presence or absence of sunitinib treatment. Indeed, quantitative gene expression data

showed increased gene expression of AR-driven *KLK2, KLK4, ZBTB16* and *MYC* (2-100 folds) in both 786-0R and UMRC2 cells (**Fig. 2C**). We confirmed that the several AR-driven proteins were overexpressed in sunitinib treated 786-0R and enzalutamide has an inhibitory effect (**Supplementary Fig. 3**).

AR activation in prostate cancer is generally driven by dihydrotestosterone binding, nuclear translocation, and dimerization leading to DNA binding. To determine whether AR activation required the presence of androgens, we cultured the RCC cell lines in charcoal stripped media. To our surprise, the absence of androgens did not influence the cell growth of either AR^- or AR^+ cell lines, and neither modulated AR gene expression (**Supplementary Fig. 4A, B**). To further determine the contribution of androgens to AR activity in RCC, we performed mass-spectrometry analysis on PDX (RP-R-01, RP-R-02 with acquired sunitinib resistance, and RP-R-02LM with intrinsic sunitinib resistance), and tumor cell lines (786-0, 786-0R, UMRC2 and UMRC2R), and did not detect any significant presence of either testosterone, epitestosterone or progesterone (**Supplementary Fig. 4C**). Taken together, these data suggest that AR activity in RCC following sunitinib, is likely due to ligand-independent mechanisms.

To address the potential mechanism(s) of sunitinib induced AR activation, we assessed whether there was an increase in pS81, the most commonly phosphorylated residue in AR, following sunitinib resistance. Immunofluorescence analysis revealed a significant increase in both total nuclear AR expression and pS81 AR, with sunitinib treatment in AR^+ UMRC2 and 786-0R (after sunitinib wash out) cell lines (**Fig. 2D-F**). Increased total and pS81 AR was confirmed by Western blot analysis (**Fig. 2G**). AR phosphorylation has been implicated in nuclear translocation in prostate cancer. Indeed, in 786-0, following a transient GFP-labeled AR transfection, a short treatment with sunitinib indicated a strong nuclear localization of AR (**Fig.**

2H). To determine whether the increase in CDK1 was associated with sunitinib resistance and induced AR phosphorylation, we analyzed the RP-RP-02LM tumors treated *in vivo* with sunitinib (30). Indeed, in this intrinsically sunitinib-resistant tumor, drug treatment led to increased CDK1 protein expression (**Fig. 2I**). Interestingly, we observed a similar increase of CDK1 in sunitinib-resistant 786-0R cells as compared to 786-0 cells *in vitro* (**Fig. 2J**). Taken together, these data suggest that sunitinib induces ligand-independent AR activation, and consequent nuclear translocation, likely *via* S81 phosphorylation.

Enzalutamide induces degradation of phosphorylated AR-SPOP complex. The mechanism of action of enzalutamide on AR activity in prostate cancer is primarily due to the inhibition of ligand binding to AR, which leads to the impediment of full length AR transcriptional activity. To determine the effect of enzalutamide on AR activity/expression in our system, we treated RCC cells with sunitinib, enzalutamide, or combination, and measured AR expression by immunofluorescence. As expected, baseline AR expression was high in 786-0R and UMRC2 cells, and was increased by sunitinib treatment (**Fig. 3A**). However, concomitant treatment with enzalutamide abrogated sunitinib-induced AR expression. Surprisingly, we did not notice a significant decrease in AR expression in cells treated with enzalutamide alone. To determine whether enzalutamide-induced AR inhibition was due to induced protein degradation, we ran a separate experiment where 786-0R cells were exposed to either enzalutamide, sunitinib, or combination in the presence or the absence of the proteasome inhibitor MG132. Visual and quantitative data showed no significant decrease in AR expression with enzalutamide, or combination treatment, in the presence of MG132, suggesting that enzalutamide induced AR degradation in the presence of sunitinib (**Fig. 3B, C**). AR modulation was confirmed by Western

blotting (**Supplementary Fig. 5**). AR rescued degradation by MG132 in the presence of sunitinib and enzalutamide was associated with restoration of cell proliferation, as suggested by Ki67 staining (**Supplementary Fig. 6**). Next, we investigated the potential mechanism by which enzalutamide induces AR degradation in sunitinib treated RCC cells. Cullin-RING ligases (CRLs) complexes, specifically CRL3 complex, have been identified as *bona fide* ubiquitination ligases of AR (31,32). Thus, we performed Western blot analysis in our RCC lines to determine the level of SPOP expression (**Supplementary Fig. 7A**). We then performed a transient SPOP knockdown in UMRC2 cells, which expressed the highest levels of SPOP compared to other RCC cell lines. Upon confirmation of successful knockdown (**Supplementary Fig. 7B**), we analyzed the effect of SPOP siRNA on AR modulation. In the presence of sunitinib, there was a significant increased AR expression in UMRC2siSPOP cells as compared to UMRC2, while enzalutamide failed to abrogate this surge in UMRC2siSPOP cells (**Fig. 3D, E**). We confimed the effect of SPOP by using a different siRNA (**Supplementary Fig. 7C, D).** The lack of AR degradation induced by enzalutamide in UMRC2siSPOP cells in the presence of sunitinib, was associated with loss of the anti-proliferative effect of this combination (**Fig. 3F, G**). Interestingly, rescued enzalutamide-induced AR degradation by siSPOP was not associated with restored global serine and tyrosine phosphorylation in the presence of sunitinib, suggesting that AR phosphorylation and activation may be part of an epigenetic reprogramming but it does not affect global protein phosphorylation (28) (**Supplementary Fig. 8A, B**). Overall, these data suggest that SPOP may mediate enzalutamide-induced AR degradation, primarily in the presence of sunitinib in RCC. To further investigate the mechanisms responsible for enzalutamide-induced AR degradation, we assessed the interaction of AR and ubiquitin in 786-0R cells treated with sunitinib, following drug wash-out. Indeed, immunoprecipitation studies showed that ubiquitin

associated with AR following sunitinib treatment (**Fig. 3H**), suggesting the involvement of AR ubiquitination in its proteasome-dependent degradation.

To determine whether the effect of enzalutamide was specifically due to binding to AR, we performed a competitive assay using ddihydrotestosterone (DHT). Following drug wash-out in charcoal stripped media, 786-0R cells were exposed to DHT, and AR nuclear localization was observed (**Supplementary Fig. 9**). Sunitinib alone also induced strong AR nuclear localization which was abrogated with concomitant enzalutamide treatment. However, concomitant DHT treatment completely rescued the effect of enzalutamide on AR. Taken together, our results suggest that sunitinib induces AR phosphorylation in RCC, and upon AR binding, enzalutamide likely inhibits AR nuclear translocation that prones to SPOP-mediated AR degradation *via* the ubiquitin-proteasome pathway (**Fig. 3I**) (Supplementary Video 1 and 2).

Enzalutamide restores sunitinib sensitivity *in vivo* and induces tumor regression in 786-0. To test the effectiveness of sunitinib in combination with enzalutamide *in vivo*, we performed independent experiments using the 786-0 (sunitinib sensitive) RCC model. In the first experiment, we wanted to determine whether the combination of sunitinib and enzalutamide delayed sunitinib-resistance. We implanted 786-0 tumor pieces subcutaneously into male mice, and, once tumors reached an average size of $100mm^3$, we started treatment with either sunitinib, enzalutamide, or combination. We observed a significant delay in acquired resistance to sunitinib in the combination treatment group, without over toxicities (**Fig. 4A; Supplementary Fig. 10A, B)**. Endpoint tumor weights indicated no significant changes in tumor burden within single agent groups, but a significant decrease in the combination group ($p>0.001$). Next, we wanted to investigate the effect of enzalutamide and sunitinib in combination, after tumors acquired

sunitinib resistance. We implanted 786-0 (sunitinib sensitive) tumors, and when tumors were established, and reached an average size of 150mm^3, we randomly grouped the mice into 2 initial groups, control (n=10) and sunitinib treatment (n=20). We began sunitinib treatment and observed tumor growth until day 45, when tumors became resistant to sunitinib (≥50% increase volume from nadir) (**Fig. 4B**). Then, mice in the sunitinib group were further sub-grouped into either sunitinib *plus* enzalutamide treatment arm (n=10) or enzalutamide treatment arm (n=10). Tumor growth curves and endpoint tumor weights indicate that tumors in mice treated with sunitinib *plus* enzalutamide regressed in size, compared to single agent enzalutamide (**Fig. 4B**). Furthermore, assessment of AR pSer81 expression across treatment groups showed an increase with sunitinib resistance, as compared to the control and the combination treatment group (**Fig. 4C**). Decreased AR pSer81 expression in the combination group was associated with increased apoptosis (TUNEL) (**Fig. 4D**). Despite inhibition of angiogenesis (CD31 staining), sunitinib-resistant tumor cells continued to proliferate *in vivo* (Ki67 staining), though the combination group showed the lowest proliferation rate (**Fig. 4E, F**).

Circulating human kallikrein 2 is modulated by sunitinib and enzalutamide in RCC. In our original screening of AR target genes, we observed that human kallikrein 2 (*hK2* or KLK2) and human kallikrein4 (*hK4* or KLK4*)* were increased in 786-R cells. Thus, we decided to measure KLK2 in our models. To determine whether we were effectively inhibiting AR activity with enzalutamide treatment, we measured KLK2 in conditioned media from our *in vitro* studies, and in serum from our *in vivo* studies, by using a human KLK2 ELISA kit. We were able to detect circulating KLK2 in the 786-0 model, and the levels were decreased in the enzalutamide treated mice, and more significantly in the combination group (**Fig. 5A**). In tissue culture supernatants,

the amount of KLK2 was associated with AR status in RCC cell lines (**Fig. 5B**), was *in vitro* modulated by enzalutamide (**Fig. 5C**), and was increased in the serum in our sunitinib acquired

(RP-R-R02) and intrinsic (RP-R-02LM) resistance models (**Fig. 5D**). Interestingly, in a small number of patients enrolled in our Phase I clinical trial with sunitinib and deltaparin (33), ccRCC patients who had disease progression, presented increased serum levels KLK2, as compared to non-progressors (defined as patients with either stable disease or objective response as best response) following 3 months treatment (**Fig. 5E, F**) .

Discussion

Our study identified AR expression to be significantly increased across sunitinib resistant RCC models. We report that sunitinib induces AR activity, *via* AR S81 phosphorylation and consequent nuclear translocation. Furthermore, enzalutamide-induced degradation of phosphorylated AR leads to restoration of sunitinib sensitivity in RCC models, both *in vitro* and *in vivo*. These findings provide a rationale for the clinical testing of combination strategies with AR and RTK inhibitors in RCC.

We have recently reported that sunitinib resistance induces epigenetic-driven kinome reprogramming in RCC models, leading to increased global serine and tyrosine phosphorylation (28). In view of these findings, we hypothesized that the increased AR activation/expression, initially observed in our sunitinib-resistant PDX model by RPPA, was due to the phosphorylation of AR from sunitinib-induced kinase activation. Post-translational modifications have been reported to regulate AR activity (34). Indeed, our *in vitro* and *in vivo* data indicate that RCC cells exposed to sunitinib show increased serine 81 phosphorylated AR. There is evidence that Src activation is one of the alternative pathways induced by RTKi resistance (28) (35), and this kinase is involved in AR phosphorylation (13). Our data suggest that CDK1 may also be induced upon sunitinib resistance. Thus, following chronic exposure to RTKi and consequent acquired resistance, there may be converging pathways leading to AR phosphorylation *via* kinome reprogramming in RCC (28).

The well-established mode of AR inhibition in prostate cancer is through the blockage of DHT-AR binding and/or androgen synthesis (36-38). Enzalutamide, a well-established AR antagonist, has been reported to inhibit AR activity in prostate cancer primarily *via* competition with ligand binding, inhibition of AR nuclear translocation and chromatin binding. Based on the

results suggesting increased AR activity in resistant cells with sunitinib exposure, we assessed the combination effect of enzalutamide and sunitinib in resistant RCC models. Thus, we observed a significant inhibitory effect on cell viability in the combination group, as compared to cells treated with single agents. Most interestingly, our *in vivo* data showed a regression of tumor growth with the combination treatment. Cullin-RING ligases (CRLs) complexes, specifically the CRL3 complex, have been identified as ubiquitination ligases of AR (31,32). The complex includes the SPOP adapter, a BTB (Bric-a-brac/Tramtrack/broad complex) domain protein that recognizes the SPOP binding motif harbored in wild type AR and promotes AR degradation, and consequently, inhibition of AR transcriptional activity in prostate cancer. SPOP mediated degradation is further enhanced in the presence of enzalutamide (39). Thus, SPOP has been reported to be a tumor suppressor gene in prostate cancer, and its mutations have been involved in enzalutamide resistance (40) (41). In contrast, SPOP has also been implicated in RCC progression, but its role, with respect to AR signaling, has not been assessed (42,43). Our data in RCC models suggest that enzalutamide-induced AR degradation, primarily in the presence of sunitinib, occurs *via* the anchoring of SPOP on AR. Immunoprecipitation studies also suggest that ubiquitin is associated with AR, following sunitinib treatment. Thus, we hypothesize that post-translational modifications induced by chronic exposure to sunitinib and binding to enzalutamide, induce AR conformational changes that facilitate AR cytoplasmic retention and SPOP-ubiquitin-proteasome-dependent degradation, with subsequent inhibition of previously activated AR-driven survival pathways. Further mechanistic studies will be necessary to identify whether AR phosphorylation occurs at additional critical residues, and which survival signalings are involved.

The treatment of RCC is rapidly evolving, but RTKis remain the standard of care. However, acquired drug resistance represents a major hurdle. Effective therapeutic strategies to overcome/delay resistance have not been developed yet. AR has been previously reported to be expressed in RCC, and has been identified as a potential therapeutic target (4) (5). Interestingly, under our experimental conditions, single agent enzalutamide did not elicit a significant anti-tumor effect in AR-expressing RCC models. However, the concomitant presence of sunitinib and consequent phosphorylation of AR, induced inhibition of cell proliferation and apoptosis. This observation would suggest that AR signaling may act primarily as a survival pathway in the context of kinome reprogramming in RCC. Thus, we believe that the clinical development of AR antagonists as single agent modality in RCC patients, may fail to achieve a meaningful clinical outcome, unless paired with RTKis. The clinical testing of this combination strategy will need to also take into account the potential drug-drug interaction between these agents, since sunitinib, for example, is metabolized predominantly by the hepatic cytochrome P450 enzyme CYP3A4 (44). Enzalutamide is a strong CYP3A4 inducer and could decrease patient exposure to sunitinib, thus requiring a dose-adjustment (45).

In our analysis of AR target genes, we observed that KLK2 and KLK4 were among the top 10 genes increased in 786-R cells. Interestingly, KLK3 (or PSA) was not expressed, likely due to epigenetic silencing. Thus, we decided to measure KLK2 in our models, since KLK2 is a secreted kallikrein and is measurable in patients with prostate cancer (4K score test). Our preliminary data are intriguing because they suggest a correlation between levels of KLK2 and the presence of an activated AR pathway. More interestingly, in a small cohort of RCC patients who were treated with sunitinib KLK2 was induced in patients whose disease has progressed but not in those with an objective response. If confirmed in future studies, we hypothesize that

measuring circulating levels of KLK2 may not only predict whether a patient will respond to RTKis, but will also help to determine when the tumor is becoming resistant. This potential biomarker will also be helpful to monitor disease response to AR and RTK inhibitors.

Taken together, our data suggest that post-translational modifications of AR may modulate sunitinib resistance in RCC, and may be targeted by enzalutamide treatment *via* SPOP-mediated degradation. In conclusion, our work provides important molecular insights in RTKi resistance RCC, and identifies AR protein and a circulating AR-modulated kallikrein as potential therapeutic target and predictive marker, respectively, for this disease, and potentially other solid tumors where AR has been reported to be biologically active, such as lung and breast cancer (3) (46).

Acknowledgments

This research was in part funded by the Roswell Park Cancer Institute Cancer Center Support Grant (P30CA016056) (R. Pili), from the National Cancer Institute, and a generous donation by Richard and Deidre Turner (R. Pili). This investigation was conducted in part, in a facility constructed with support from Research Facilities Improvement Program Grant Number C06 RR020128-01 from the National Center for Research Resources, National Institutes of Health.

REFERENCES

1. Schweizer MT, Yu EY. AR-Signaling in Human Malignancies: Prostate Cancer and Beyond. Cancers (Basel) **2017**;9
2. Berardi R, Morgese F, Santinelli A, Onofri A, Biscotti T, Brunelli A, *et al.* Hormonal receptors in lung adenocarcinoma: expression and difference in outcome by sex. Oncotarget **2016**;7:82648-57
3. Yenerall P, Kittler R. Minireview: Familiar Faces in Unfamiliar Places: The Emerging Role of Nuclear Receptors in Lung Cancer. Mol Endocrinol **2015**;29:1675-83
4. Zhu G, Liang L, Li L, Dang Q, Song W, Yeh S, *et al.* The expression and evaluation of androgen receptor in human renal cell carcinoma. Urology **2014**;83:510 e19-24
5. He D, Li L, Zhu G, Liang L, Guan Z, Chang L, *et al.* ASC-J9 suppresses renal cell carcinoma progression by targeting an androgen receptor-dependent HIF2alpha/VEGF signaling pathway. Cancer Res **2014**;74:4420-30
6. Kameyama K, Horie K, Mizutani K, Kato T, Fujita Y, Kawakami K, *et al.* Enzalutamide inhibits proliferation of gemcitabine-resistant bladder cancer cells with increased androgen receptor expression. Int J Oncol **2017**;50:75-84
7. Guan Z, Li C, Fan J, He D, Li L. Androgen receptor (AR) signaling promotes RCC progression via increased endothelial cell proliferation and recruitment by modulating AKT --> NF-kappaB --> CXCL5 signaling. Sci Rep **2016**;6:37085
8. Zhao H, Leppert JT, Peehl DM. A Protective Role for Androgen Receptor in Clear Cell Renal Cell Carcinoma Based on Mining TCGA Data. PLoS One **2016**;11:e0146505
9. Anbalagan M, Huderson B, Murphy L, Rowan BG. Post-translational modifications of nuclear receptors and human disease. Nucl Recept Signal **2012**;10:e001
10. Koryakina Y, Ta HQ, Gioeli D. Androgen receptor phosphorylation: biological context and functional consequences. Endocr Relat Cancer **2014**;21:T131-45
11. Zhou ZX, Kemppainen JA, Wilson EM. Identification of three proline-directed phosphorylation sites in the human androgen receptor. Mol Endocrinol **1995**;9:605-15
12. Chattopadhyay I, Wang J, Qin M, Gao L, Holtz R, Vessella RL, *et al.* Src promotes castration-recurrent prostate cancer through androgen receptor-dependent canonical and non-canonical transcriptional signatures. Oncotarget **2017**;8:10324-47
13. Gelman IH. Androgen receptor activation in castration-recurrent prostate cancer: the role of Src-family and Ack1 tyrosine kinases. Int J Biol Sci **2014**;10:620-6
14. Chen S, Xu Y, Yuan X, Bubley GJ, Balk SP. Androgen receptor phosphorylation and stabilization in prostate cancer by cyclin-dependent kinase 1. Proc Natl Acad Sci U S A **2006**;103:15969-74
15. Lin HK, Hu YC, Yang L, Altuwaijri S, Chen YT, Kang HY, *et al.* Suppression versus induction of androgen receptor functions by the phosphatidylinositol 3-kinase/Akt pathway in prostate cancer LNCaP cells with different passage numbers. J Biol Chem **2003**;278:50902-7
16. Lee SH, Johnson D, Luong R, Sun Z. Crosstalking between androgen and PI3K/AKT signaling pathways in prostate cancer cells. J Biol Chem **2015**;290:2759-68
17. Ha S, Ruoff R, Kahoud N, Franke TF, Logan SK. Androgen receptor levels are upregulated by Akt in prostate cancer. Endocr Relat Cancer **2011**;18:245-55
18. Mitsiades N. A road map to comprehensive androgen receptor axis targeting for castration-resistant prostate cancer. Cancer Res **2013**;73:4599-605

19. Stone L. Kidney cancer: Path to progression: intracrine signalling in RCC. Nat Rev Urol **2017**
20. Tran C, Ouk S, Clegg NJ, Chen Y, Watson PA, Arora V, *et al.* Development of a second-generation antiandrogen for treatment of advanced prostate cancer. Science **2009**;324:787-90
21. Scher HI, Fizazi K, Saad F, Taplin ME, Sternberg CN, Miller K, *et al.* Increased survival with enzalutamide in prostate cancer after chemotherapy. N Engl J Med **2012**;367:1187-97
22. Albiges L, Choueiri T, Escudier B, Galsky M, George D, Hofmann F, *et al.* A systematic review of sequencing and combinations of systemic therapy in metastatic renal cancer. Eur Urol **2015**;67:100-10
23. Choueiri TK, Escudier B, Powles T, Mainwaring PN, Rini BI, Donskov F, *et al.* Cabozantinib versus Everolimus in Advanced Renal-Cell Carcinoma. N Engl J Med **2015**;373:1814-23
24. Schuller H, Leipner N, Rollmann O, Harder T. [A procedure for taking into account scattered radiation and scattered light in the densitometric determination of intravascular iodine content]. Rofo **1987**;147:207-12
25. Motzer RJ, Hutson TE, Glen H, Michaelson MD, Molina A, Eisen T, *et al.* Lenvatinib, everolimus, and the combination in patients with metastatic renal cell carcinoma: a randomised, phase 2, open-label, multicentre trial. Lancet Oncol **2015**;16:1473-82
26. Jayson GC, Kerbel R, Ellis LM, Harris AL. Antiangiogenic therapy in oncology: current status and future directions. Lancet **2016**;388:518-29
27. Zhou L, Liu XD, Sun M, Zhang X, German P, Bai S, *et al.* Targeting MET and AXL overcomes resistance to sunitinib therapy in renal cell carcinoma. Oncogene **2016**;35:2687-97
28. Adelaiye-Ogala R, Budka J, Damayanti NP, Arrington J, Ferris MW, Hsu CC, *et al.* EZH2 modifies sunitinib resistance in renal cell carcinoma by kinome reprogramming. Cancer Res **2017**
29. Liu S, Sjovall J, Griffiths WJ. Analysis of oxosteroids by nano-electrospray mass spectrometry of their oximes. Rapid Commun Mass Spectrom **2000**;14:390-400
30. Adelaiye R, Ciamporcero E, Miles KM, Sotomayor P, Bard J, Tsompana M, *et al.* Sunitinib dose escalation overcomes transient resistance in clear cell renal cell carcinoma and is associated with epigenetic modifications. Molecular cancer therapeutics **2015**;14:513-22
31. Li C, Ao J, Fu J, Lee DF, Xu J, Lonard D, *et al.* Tumor-suppressor role for the SPOP ubiquitin ligase in signal-dependent proteolysis of the oncogenic co-activator SRC-3/AIB1. Oncogene **2011**;30:4350-64
32. Gan W, Dai X, Lunardi A, Li Z, Inuzuka H, Liu P, *et al.* SPOP Promotes Ubiquitination and Degradation of the ERG Oncoprotein to Suppress Prostate Cancer Progression. Mol Cell **2015**;59:917-30
33. Wentink MQ, Verheul HMW, Pal SK, George S, Voortman J, Danchaivijitr P, *et al.* Phase I Study of Dalteparin in Combination With Sunitinib in Patients With Metastatic Clear Cell Renal Carcinoma. Clin Genitourin Cancer **2017**
34. van der Steen T, Tindall DJ, Huang H. Posttranslational modification of the androgen receptor in prostate cancer. Int J Mol Sci **2013**;14:14833-59

35. Bai L, Yang JC, Ok JH, Mack PC, Kung HJ, Evans CP. Simultaneous targeting of Src kinase and receptor tyrosine kinase results in synergistic inhibition of renal cell carcinoma proliferation and migration. Int J Cancer **2012**;130:2693-702
36. Rathkopf D, Scher HI. Androgen receptor antagonists in castration-resistant prostate cancer. Cancer J **2013**;19:43-9
37. Tan MH, Li J, Xu HE, Melcher K, Yong EL. Androgen receptor: structure, role in prostate cancer and drug discovery. Acta Pharmacol Sin **2015**;36:3-23
38. Li H, Ban F, Dalal K, Leblanc E, Frewin K, Ma D, *et al.* Discovery of small-molecule inhibitors selectively targeting the DNA-binding domain of the human androgen receptor. J Med Chem **2014**;57:6458-67
39. An J, Wang C, Deng Y, Yu L, Huang H. Destruction of full-length androgen receptor by wild-type SPOP, but not prostate-cancer-associated mutants. Cell Rep **2014**;6:657-69
40. Geng C, Kaochar S, Li M, Rajapakshe K, Fiskus W, Dong J, *et al.* SPOP regulates prostate epithelial cell proliferation and promotes ubiquitination and turnover of c-MYC oncoprotein. Oncogene **2017**;36:4767-77
41. Blattner M, Liu D, Robinson BD, Huang D, Poliakov A, Gao D, *et al.* SPOP Mutation Drives Prostate Tumorigenesis In Vivo through Coordinate Regulation of PI3K/mTOR and AR Signaling. Cancer Cell **2017**;31:436-51
42. Zhao W, Zhou J, Deng Z, Gao Y, Cheng Y. SPOP promotes tumor progression via activation of beta-catenin/TCF4 complex in clear cell renal cell carcinoma. Int J Oncol **2016**;49:1001-8
43. Guo ZQ, Zheng T, Chen B, Luo C, Ouyang S, Gong S, *et al.* Small-Molecule Targeting of E3 Ligase Adaptor SPOP in Kidney Cancer. Cancer Cell **2016**;30:474-84
44. Rock EP, Goodman V, Jiang JX, Mahjoob K, Verbois SL, Morse D, *et al.* Food and Drug Administration drug approval summary: Sunitinib malate for the treatment of gastrointestinal stromal tumor and advanced renal cell carcinoma. Oncologist **2007**;12:107-13
45. Gibbons JA, de Vries M, Krauwinkel W, Ohtsu Y, Noukens J, van der Walt JS, *et al.* Pharmacokinetic Drug Interaction Studies with Enzalutamide. Clin Pharmacokinet **2015**;54:1057-69
46. Kono M, Fujii T, Lim B, Karuturi MS, Tripathy D, Ueno NT. Androgen Receptor Function and Androgen Receptor-Targeted Therapies in Breast Cancer: A Review. JAMA Oncol **2017**;3:1266-73

FIGURE LEGEND

Figure 1: Sunitinib resistance is associated with increased AR expression, and AR inhibition restores drug sensitivity in RCC models. (A) RPPA data indicate increased AR expression in RP-R-01 RCC PDX model at the time of resistance. (B) Immunohistochemistry and (C) qRT-PCR analysis indicating AR expression in RCC PDX models sensitive (*ss*) and resistant (*sr*) to sunitinib. (D-F) mRNA, Western blot analysis and proliferation assay on RCC cell lines, indicate increased AR expression in tumor cells that are less sensitive to sunitinib. IC50 for sunitinib correlates with AR status. (G) Cell viability assay of RCC cell lines treated with either sunitinib, enzalutamide or combination, for 48hrs indicates synergistic decrease in cell viability in the combination group, only in the presence of AR expression. (H) Ki67 immunofluorescence staining and quantitation of 786-0R cells treated with either sunitinib, enzalutamide or combination. (I) Proliferation assay with different sunitinib concentrations shows the shift in IC50 between AR expressing 786-0 cell (786-0AR), compared to parental cell line. Bar graphs represent the mean ± SD. *$p<0.05$, **$p<0.0016$, ***$p<0.0009$, ****$p<0.0001$, ns= not significant.

Figure 2: Increased sunitinib-induced AR expression is associated with activation of AR targeted genes and increased AR phosphorylation. (A) Heatmap indicates increased expression of AR target genes in resistant cells compared to the parental 786-0 cell line. (B) Top selected genes increased with increased AR. (C) q-PCR analysis shows modulation of AR targeted genes (*KLK2*, *KLK4*, *ZBTB16*, *MYC*) in AR^+ 786-0R and UMRC2 cell lines, following exposure to sunitinib (48hrs). (D) Immunofluorescence staining for AR phospho Ser 81 and AR-

C terminal domain in UMRC2 and 786-0R (after 3-4 weeks washout), following exposure to sunitinib (48hrs). Immunofluorescence includes F-actin (green) and Hoechst (blue) staining for cytoplasm and nuclear visualization, respectively. (E, F) Quantitative analysis by Image J. (G) Western blot analysis for AR pSer81 and AR-C terminal domain. (H) GFP-labelled AR expressed in 786-0 cell: Nuclear protein localization following short exposure (45 minutes) to sunitinib. (I) Western blot analysis for CDK1 expression in RP-R-R02LM tumors, following sunitinib exposure *in vivo*. (J) CDK1 protein expression by Western blot analysis in 786-0 cell line is increased in sunitinib-resistant 786-0R *in vitro*. Bar graphs represent the mean ± SD. ****$p<0.0001$.

Figure 3: Sunitinib-induced AR expression is antagonized by enzalutamide *via* SPOP-mediated proteasome protein degradation. (A) Immunofluorescence quantitative analysis of AR expression in 786-0, 786-0R, and UMRC2 cell lines treated with sunitinib, enzalutamide, or combination. (B, C) Immunofluorescence staining and quantitative analysis of AR-N terminal domain (red) in 786-0R treated with sunitinib and enzalutamide and combination ± the proteasome inhibitor MG132. Immunofluorescence includes F-actin (green) and Hoechst (blue) staining for cytoplasm and nuclear visualization, respectively. (D, E) Immunofluorescence staining and quantitative analysis of AR-N terminal domain in UMRC2 and UMRC2siSPOP, following exposure to sunitinib, enzalutamide, or combination. (F, G) Proliferation assay in UMRC2 and UMRC2siSPOP cells treated with sunitinib, enzalutamide, or combination. The inhibition of SPOP neutralizes the antitumor effect of enzalutamide in the presence of sunitinib. (H) Immunoprecipitation of AR and ubiquitin in 786-0R ± sunitinib suggesting increased drug-induced AR ubiquitination. (I) Graphical presentation of the proposed mechanism(s) responsible

for sunitinib-induced AR activation and enzalutamide-induced AR degradation**.** Bar graphs represent the mean ± SD. *p<0.05, **p<0.001, ***p<0.005, ****p<0.0001, ns= not significant.

Figure 4: Enzalutamide restores sensitivity to sunitinib *in vivo*. (A) NSG mice carrying established 786-0 tumors were treated with sunitinib, and enzalutamide. Tumor growth curves and end-point tumor weights are reported. (B) In a separate experiment NSG mice carrying established 786-0 tumors were treated initially with sunitinib until disease progression (≥50% tumor volume from baseline). Then, mice were randomized to enzalutamide or combination. Tumor growth curves and end-point tumor weights are reported. (C, D) Immunofluorescence staining and quantitative analysis for pAR Ser-81 and for TUNEL (apoptosis) are depicted. (E, F) Quantitative analysis for blood vessel density (CD31) and tumor cell proliferation (Ki67) are depicted. Bar graphs represent the mean ± SD. *p<0.05, **p<0.001, ***p<0.005, ****p<0.0001.

Figure 5: Circulating KLK2 as a biomarker for AR expression in RCC. (A) Quantitative analysis of end-point KLK2 serum levels by ELISA in 786-0 tumor bearing animals treated with sunitinib, enzalutamide, or combination (from Fig. 4A) is reported. (B) qRT-PCR assessment of *hk2* expression from tissue culture supernatants correlated with AR status in RCC cell lines (from Fig. 1). (C) ELISA assessment of circulating KLK2 in vitro from tissue culture supernatant treated with either sunitinib or enzalutamide, indicates increased KLK2 with sunitinib, which is altered with in the presence of enzalutamide. (D) *in vivo* data in RCC PDX model of sunitinib acquired resistance (RP-R-02) and intrinsic resistance (RP-R-02LM), indicates increased KLK2 serum concertation with sunitinib treatment. Data is represented as the mean +/- SEM (n=3). (E) Circulating KLK2 expression in serum of patients who progressed, indicates increased KLK2

compared to non-progressors (F). Bar graphs represent the mean ± SD. *p<0.05, **p<0.001, ***p<0.005, ****p<0.0001.

Suntinib Resistance Studies

gure 1

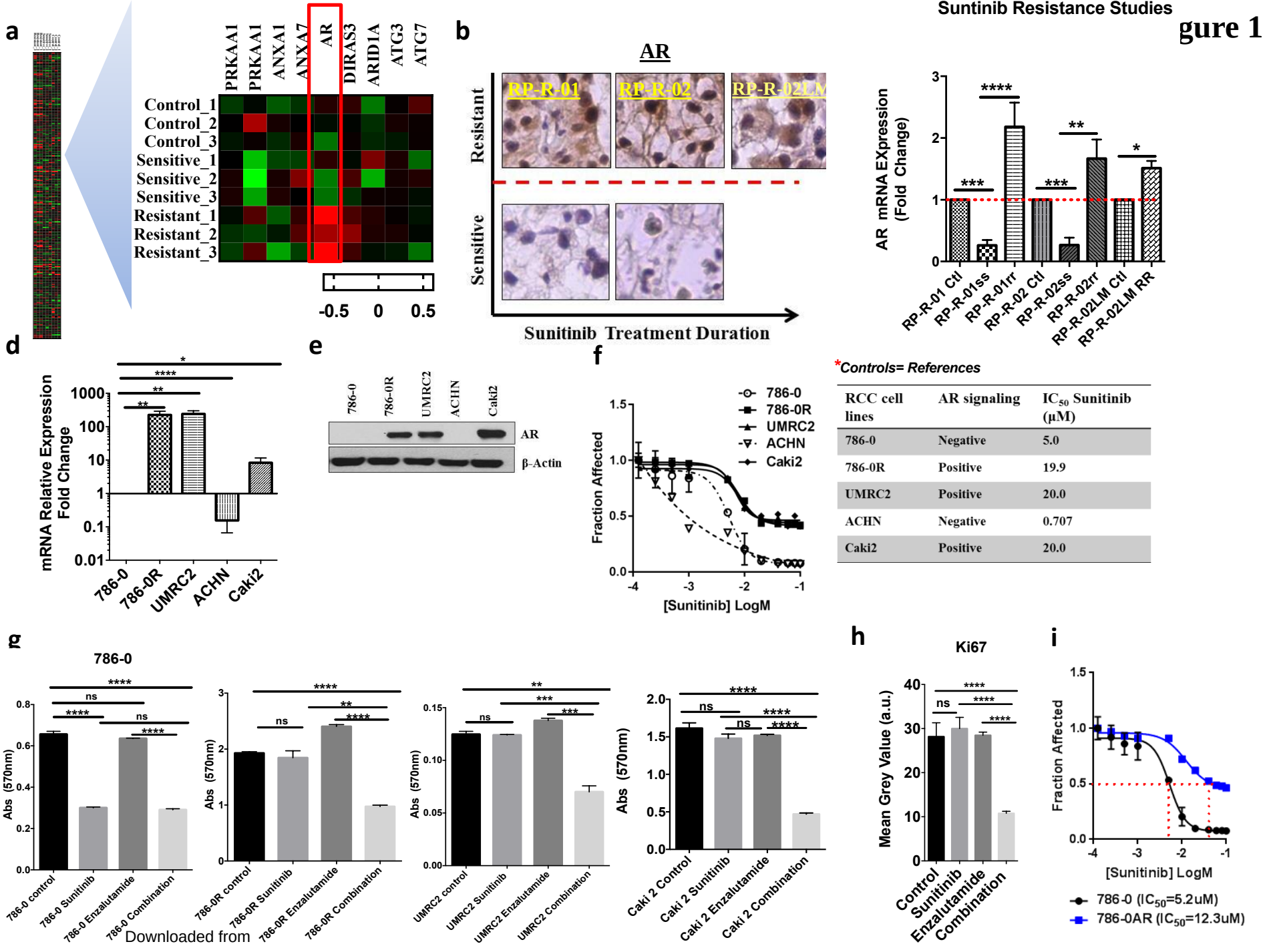

*Controls= References

RCC cell lines	AR signaling	IC_{50} Sunitinib (μM)
786-0	Negative	5.0
786-0R	Positive	19.9
UMRC2	Positive	20.0
ACHN	Negative	0.707
Caki2	Positive	20.0

Figure 2

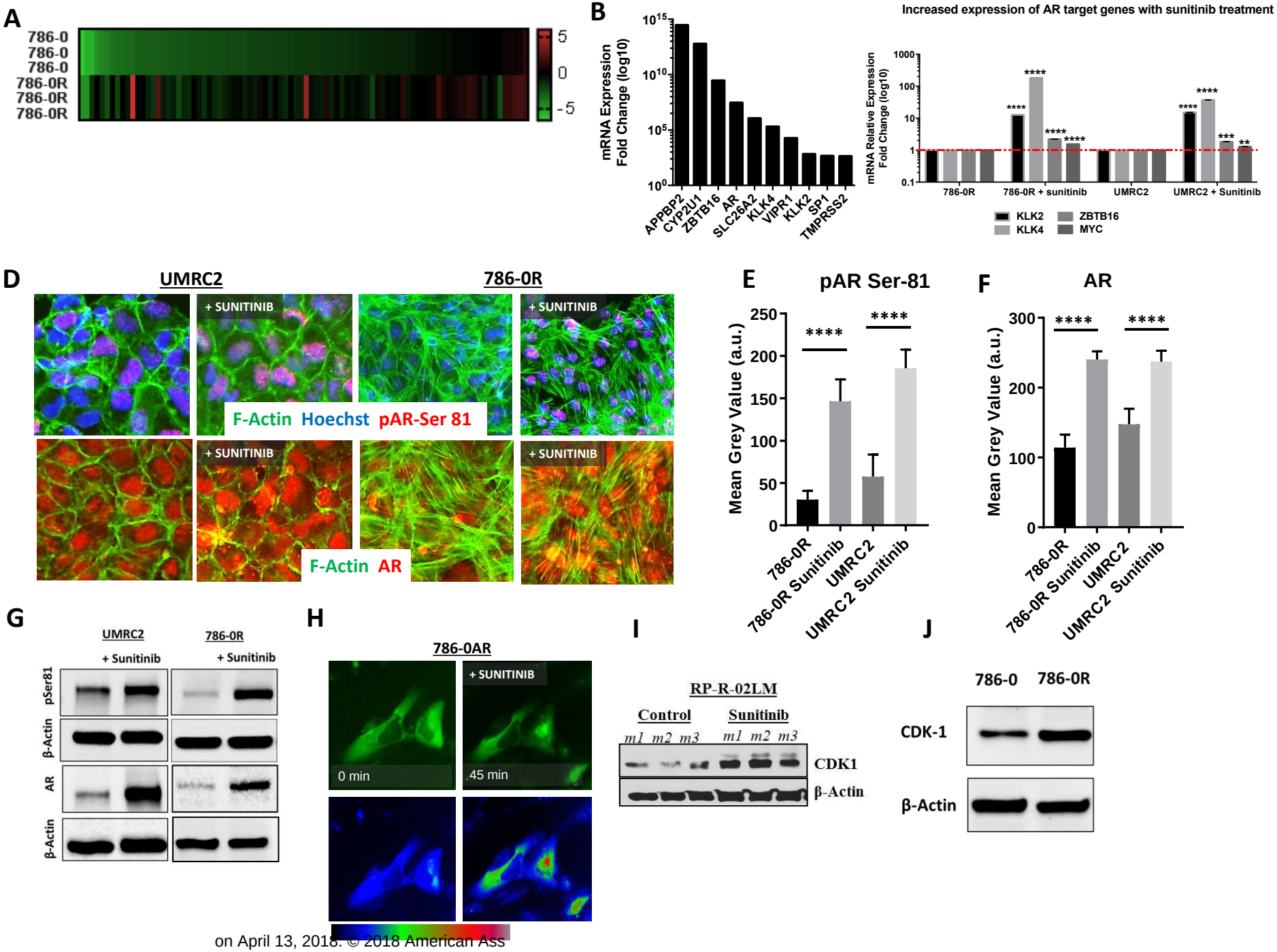

Figure 3

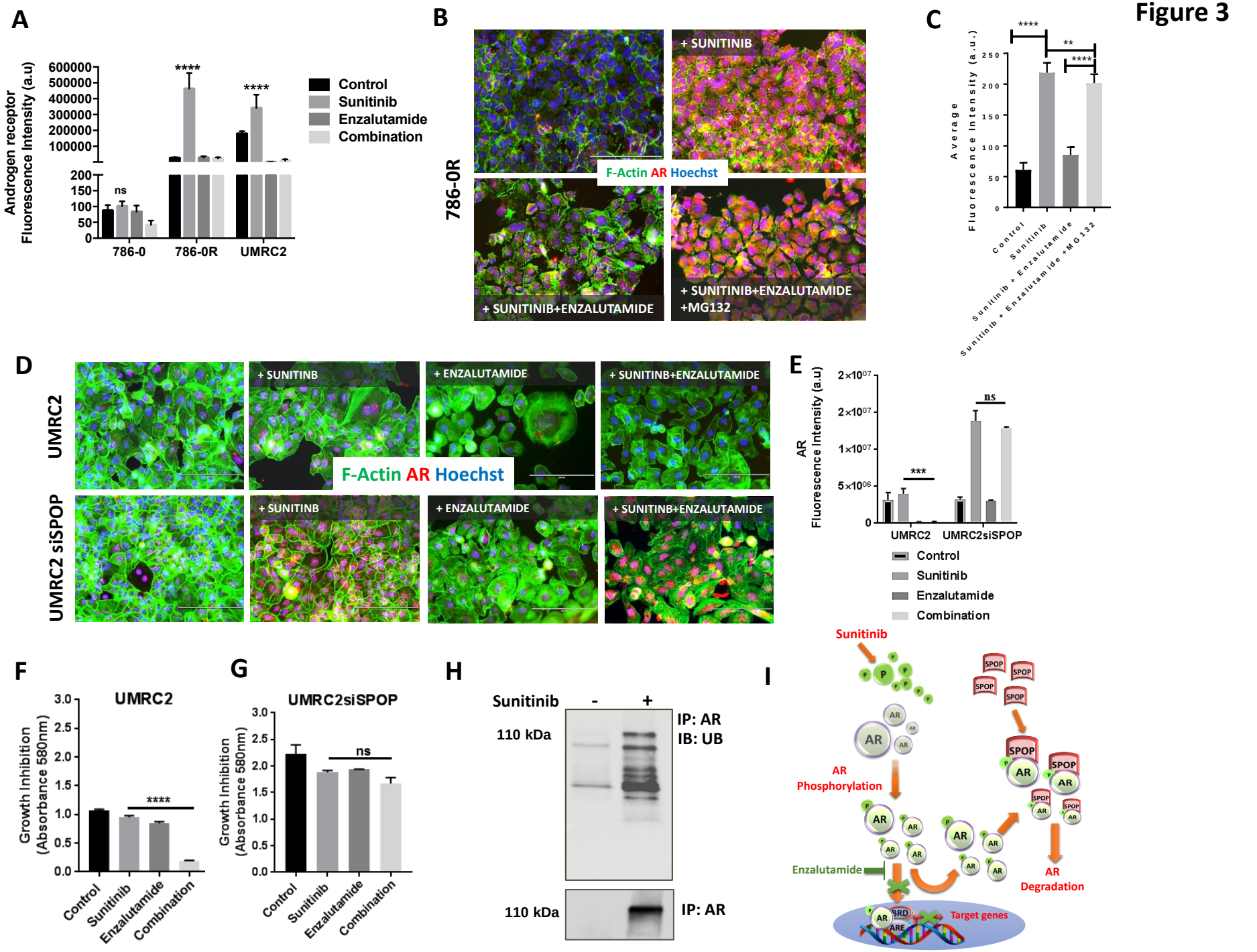
A
Androgen receptor Fluorescence Intensity (a.u)
600000
500000
400000
300000
200000
100000
200
150
100
50
0
ns
****
****
786-0
786-0R
UMRC2
Control
Sunitinib
Enzalutamide
Combination
B
786-0R
+ SUNITINIB
F-Actin AR Hoechst
+ SUNITINIB+ENZALUTAMIDE
+ SUNITINIB+ENZALUTAMIDE +MG132
C
Average Fluorescence Intensity (a.u.)
250
200
150
100
50
0
****
**
****
Control
Sunitinib
Sunitinib + Enzalutamide
Sunitinib + Enzalutamide +MG132
D
UMRC2
UMRC2 siSPOP
+ SUNITINB
+ ENZALUTAMIDE
+ SUNITINB+ENZALUTAMIDE
F-Actin AR Hoechst
E
AR Fluorescence Intensity (a.u)
2×10^07
2×10^07
1×10^07
5×10^06
0
***
ns
UMRC2
UMRC2siSPOP
Control
Sunitinib
Enzalutamide
Combination
F
UMRC2
Growth Inhibition (Absorbance 580nm)
3.0
2.5
2.0
1.5
1.0
0.5
0.0
****
Control
Sunitinib
Enzalutamide
Combination
G
UMRC2siSPOP
Growth Inhibition (Absorbance 580nm)
3.0
2.5
2.0
1.5
1.0
0.5
0.0
ns
Control
Sunitinib
Enzalutamide
Combination
H
Sunitinib
-
+
110 kDa
IP: AR
IB: UB
110 kDa
IP: AR
I
Sunitinib
P
SPOP
AR
AR Phosphorylation
Enzalutamide
AR Degradation
BRD
ARE
Target genes

Figure 4

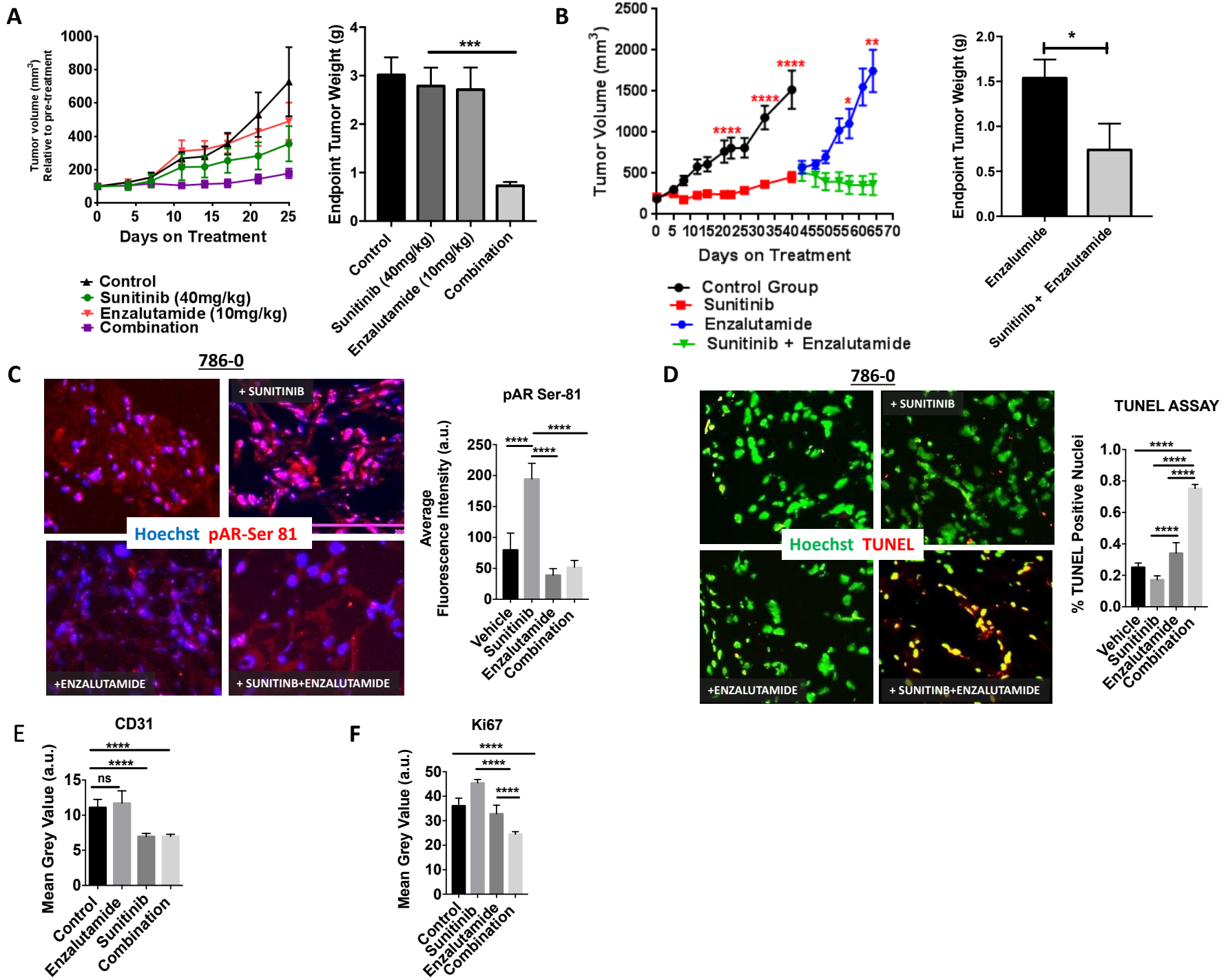
A
Tumor volume (mm3) Relative to pre-treatment
Days on Treatment
Control
Sunitinib (40mg/kg)
Enzalutamide (10mg/kg)
Combination
Endpoint Tumor Weight (g)
Control
Sunitinib (40mg/kg)
Enzalutamide (10mg/kg)
Combination
B
Tumor Volume (mm3)
Days on Treatment
Control Group
Sunitinib
Enzalutamide
Sunitinib + Enzalutamide
Endpoint Tumor Weight (g)
Enzalutmide
Sunitinib + Enzalutamide
C
786-0
+ SUNITINIB
Hoechst pAR-Ser 81
+ENZALUTAMIDE
+ SUNITINB+ENZALUTAMIDE
pAR Ser-81
Average Fluorescence Intensity (a.u.)
Vehicle
Sunitinib
Enzalutamide
Combination
D
786-0
+ SUNITINIB
Hoechst TUNEL
+ENZALUTAMIDE
+ SUNITINB+ENZALUTAMIDE
TUNEL ASSAY
% TUNEL Positive Nuclei
Vehicle
Sunitinib
Enzalutamide
Combination
E
CD31
Mean Grey Value (a.u.)
ns
Control
Enzalutamide
Sunitinib
Combination
F
Ki67
Mean Grey Value (a.u.)
Control
Sunitinib
Enzalutamide
Combination

Figure 5

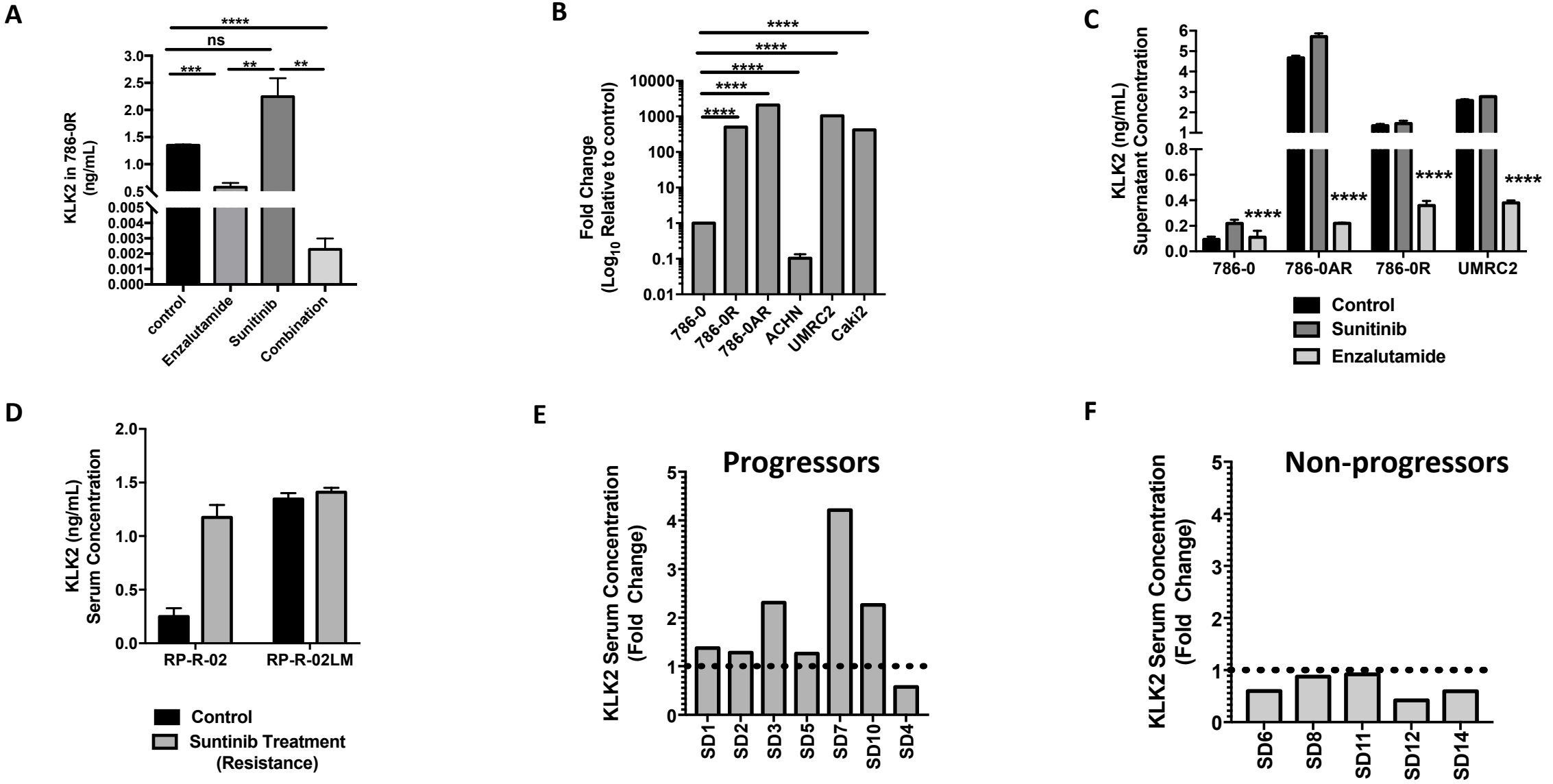
A
KLK2 in 786-0R (ng/mL)
control
Enzalutamide
Sunitinib
Combination
B
Fold Change (Log10 Relative to control)
786-0
786-0R
786-0AR
ACHN
UMRC2
Caki2
C
KLK2 (ng/mL) Supernatant Concentration
786-0
786-0AR
786-0R
UMRC2
Control
Sunitinib
Enzalutamide
D
KLK2 (ng/mL) Serum Concentration
RP-R-02
RP-R-02LM
Control
Suntinib Treatment (Resistance)
E
Progressors
KLK2 Serum Concentration (Fold Change)
SD1
SD2
SD3
SD5
SD7
SD10
SD4
F
Non-progressors
KLK2 Serum Concentration (Fold Change)
SD6
SD8
SD11
SD12
SD14